09

Raman light scattering and photoluminescence of ceria based ytterbium derivative

© S.N. Shkerin[1], O.I. Gyrdasova[2], R.K. Abdurakhimova[1], A.V. Tkachuk[1], K.V. Abasova[1]

[1] Institute of High-Temperature Electrochemistry, Ural Branch, Russian Academy of Sciences, Yekaterinburg, Russia
[2] Institute of Solid State Chemistry, Russian Academy of Sciences, Ural Branch, Yekaterinburg, Russia

E-mail: shkerin@mail.ru

Received July 7, 2025
Revised December 23, 2025
Accepted December 23, 2025

Thermolysis of formate precursor complexes in air has produced a number of derivatives of $Ce(Yb)O_2$, and for selected compositions and $Ce(Y)O_2$. All samples are characterized by a face-centered cubic structure (Fm-3m), of the fluorite type. Raman spectroscopy studies using two different sources (785 and 532 nm) made it possible to isolate structural lines and photoluminescence lines, since the structural lines do not depend on the wavelength of the radiation used. Photoluminescence is observed both from the ytterbium cation and from the intrinsic defects of the oxide lattice — anionic vacancies. A change in the local structure from fluorite to pyrochlore has been traced, it occurs in the region of 9 % of the doping cation and manifests itself not only in a change in the set of structural lines, but also in a change in the frequency of luminescence of the ytterbium cation: $2375(1)\,cm^{-1}$ for the fluorite structure at low concentrations of the additive and $2440(2)\,cm^{-1}$ for the pyrochlore structure. The latter value agrees well for derivatives based on zirconium dioxide, which also have a pyrochlore structure.

Keywords: derivatives, Raman scattering of light, structural lines, ratio of fluorite/pyrochlor structures.

DOI: 10.61011/PSS.2026.01.63254.218-25

1. Introduction

Uranium, thorium, and cerium dioxides have a face-centered cubic (FCC) fluorite-type structure even in the undoped state [1]. At the same time, materials based on zirconium dioxide (or hafnium) are known and actively used, for which the FCC structure is characteristic only at high temperatures. It is stabilized by the administration of dopants. As was recently shown, despite the fact that the long-range order corresponds to the FCC structure of the fluorite type, local symmetry turns out to be characteristic of the pyrochlore structure [2,3]. The purpose of this study is to trace, using the example of doped ceria, changes in the local structure with a change in the dopant concentration. The ytterbium cation is used as the main doping cation. A number of compositions were reproduced with yttrium cations to distinguish the luminescence properties of the ytterbium cation.

2. Experimental part

2.1. Sample preparation

A precursor synthesis method based on pyrolysis of a thermally decomposable complex salt was used for the synthesis of $Ce_{1-x}Yb_xO_{2-\delta}$ $(0 < x \leq 0.5)$. A double formate was synthesized as a complex salt with an organic ligand $Ce_{1-x}Yb_x(HCOO)_3 \cdot nH_2O$.

1. Standard stoichiometric mixtures of $Ce(NO_3)_3 \cdot 6H_2O$ (sufficient for purity analysis) and Yb_2O_3 (chemically pure, c.p.) was dissolved in 1-M solution of HNO_3 (c.p.) with constant stirring and heating to 70 °C until a homogeneous solution is formed. The solution was evaporated to wet salts $Ce_{1-x}Yb_x(NO_3)_3$.

2. 85% HCOOH formic acid was carefully added to the resulting nitrate. The ion exchange reaction occurs rapidly with abundant release of nitrogen oxide vapors. After the release of brown gas, the formation of a light yellow precipitate of double formate of the conditional composition $Ce_{1-x}Yb_x(HCOO)_3$ was observed, which was used as a precursor to obtain the final product.

3. The precursor was annealed in two steps:

• at 400 °C for 1.5 h, structural water and decomposition products of the formate group are removed;

• at 700 °C for 4 h — final derivatives formation $Ce_{1-x}Yb_xO_{2-\delta}$ $(0 < x \leq 0.5)$.

2.2. X-ray examinations

The certification and control of the phase composition of the samples was carried out by powder X-ray diffraction analysis (XDA) using a Bruker Advance D8 diffractometer in Cu-Kα-radiation ($\lambda = 1.5406$,Å). The samples were scanned at room temperature in the air in the range of $10-122°$ with an increment of $\Delta 2\theta = 0.01°$ at an angular scanning speed of 0.8 deg/min, the total number of increments was 11,000. Analysis of the phase composition

and calculation of crystallographic parameters were carried out using the Smart Lab Studio II software package based on database PDF-2 ICDD (Powder Diffraction File PDF2 ICDD Release 2019).

2.3. Chemical analysis

The chemical analysis of nominally pure ceria was performed using a Lab centerXRF-1800 X-ray fluorescence spectrometer from Shimadzu, Japan.

2.4. Studies by Raman scattering method

RS studies were carried out using Renishaw U 1000 microscope-spectrometer with two different sources:

- green radiation ($\lambda = 532$ nm); the power of the Nd:YAG laser was 50 mW;
- in red radiation ($\lambda = 785$ nm) on InVia Reflex with the microscope Leica DM2700; power of the Renishaw diode laser with an integrated plasma filter was 300 mW.

3. Results

Figure 1 shows an example of diffraction patterns for nominally pure ceria. The sample is single-phase, with a fluorite-type structure (Fm-3m), which is true for all the samples studied. The lattice parameter and the Rietveld fitting parameters are given in Table 1.

The lattice parameter decreases monotonously, which is caused by an increase in the concentration of oxygen vacancies V_o with an increase in the concentration of the doping cation by the ratio

$$2[\mathrm{Yb_{Ce}}] = [\mathrm{V_o}].$$

Table 2 presents the results of a chemical analysis of nominally pure ceria synthesized using the standard procedure described above.

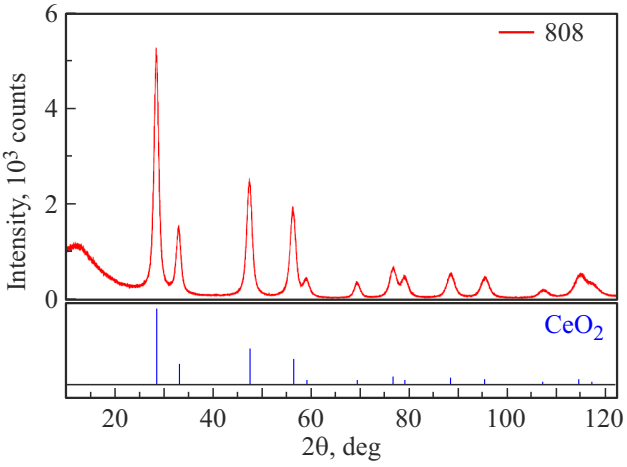

Figure 1. X-ray diffraction pattern of ceria, symmetry group Fm-3m.

Table 1. Parameters of structure refinement by the Rietveld method

C_{Yb}, %	a, Å	strain	R_{wp}, %	R_p, %	S	χ^2
0	5.41503(17)	0.60(4)	6.14	4.52	1.19	1.4162
5	5.40868(11)	0.51(3)	5.76	4.17	1.1569	1.3384
10	5.40538(13)	0.60(5)	5.13	3.70	1.0733	1.1521
23.5	5.3937(4)	0.98(10)	6.56	4.92	1.4087	1.9843
35	5.3814(3)	0.77(6)	5.42	4.24	1.2145	1.4751
43	5.3763(3)	0.86(8)	5.33	4.18	1.2506	1.5639
50	5.3682(4)	0.675(1)	5.47	4.31	1.3458	1.8111

Table 2. Results of CeO2 sample analysis by X-ray spectral fluorescence analysis

No	Name of determined element	Result of measurements, wt.%
1	Ce	99.7089
2	P	0.0911
3	Cl	0.0689
4	Ca	0.0560
5	Si	0.0489
6	S	0.0262
	Σ	100

We see the presence of small amounts of impurity cations of calcium and silicon and anions of sulfur, chlorine and phosphorus. It is important for us that they are not sources of their own luminescence.

Figure 2 shows the Raman spectra of light scattering for pure ceria obtained using a Raman spectrometer in green (532 nm) and red (785 nm) radiation. In full agreement with the literature [1], both the green and red lasers have a very intense matching line near 462 cm^{-1}.

However, in addition to the well-known very intense line, other modes are also observed. And if for the spectrum obtained in the green laser, it is necessary to reconstruct the graph with the intensity of the lines in the logarithmic axis (Figure 2, *b*) in order to see additional lines, then for the spectrum obtained in the red laser (Figure 2, *a*), their presence is obvious.

These additional lines can be attributed to a distortion of the structure [4,5], i. e., the appearance of pyrochlore lines, which is typical for doped oxide with a fluorite structure, when not only impurity cations, but also oxygen vacancies occur. Logarithmic coordinates have to be used to identify these weak lines (Figure 3).

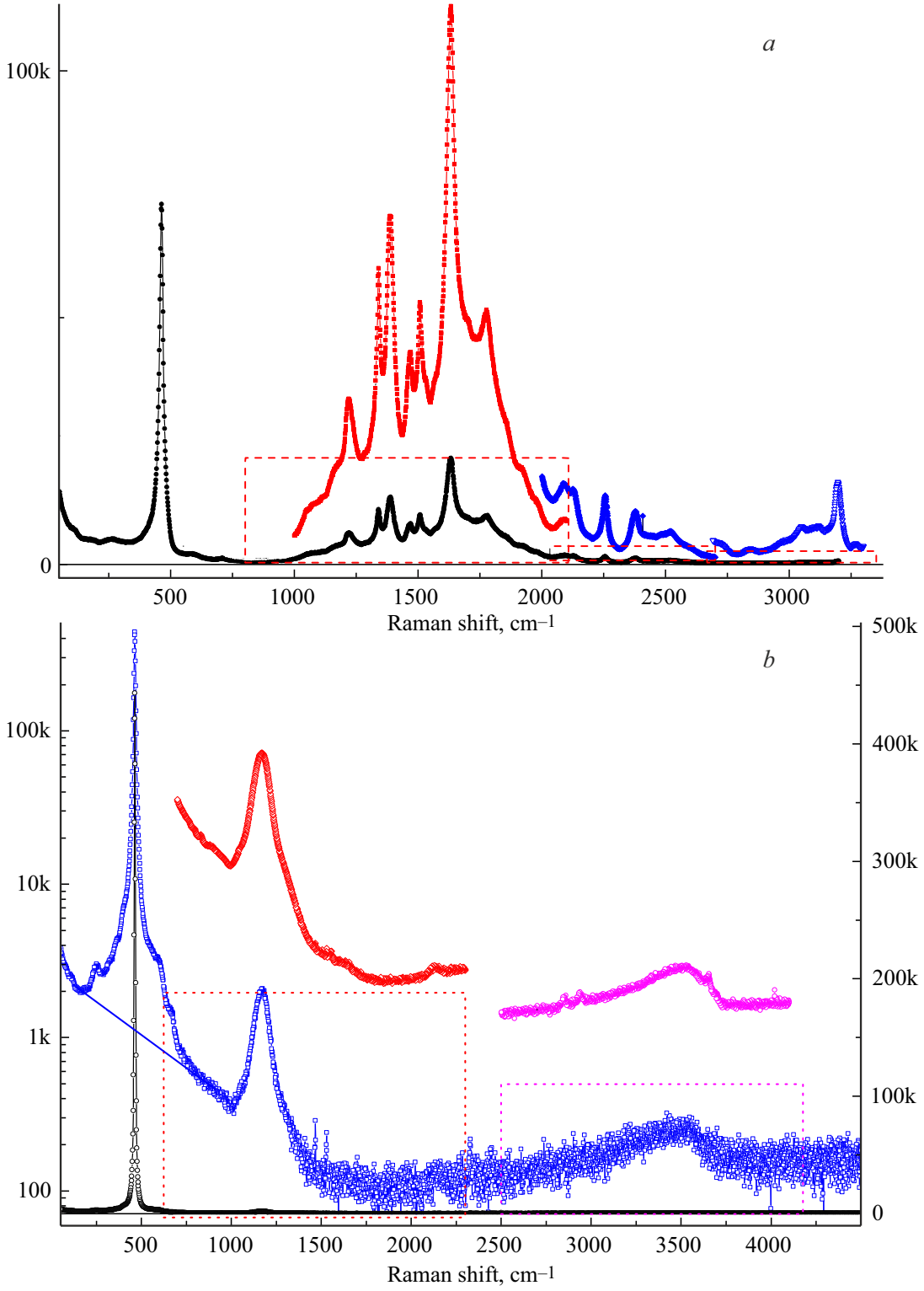

Figure 2. The spectrum of undoped ceria obtained using *a*) red (785 nm) and *b*) green (532 nm) radiation. The lines in linear intensity coordinates are represented in black. The colored lines represent the fragments of the spectrum taken with magnification.

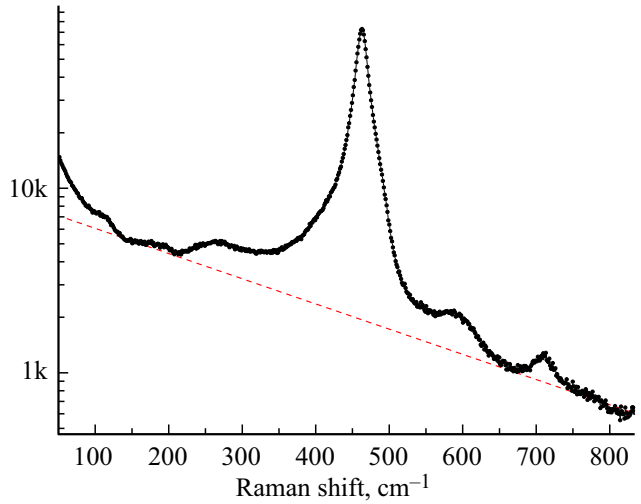

Figure 3. A fragment of the spectrum of nominally pure ceria obtained using a red (Figure 2, *a*) laser. The intensity is plotted in logarithmic coordinates, which allows you to see the presence of weak accompanying lines, as well as the asymmetry of the intense one.

On the other hand, the appearance of structural lines for the pyrochlore structure at wave numbers of more than a thousand inverse centimeters is not to be expected. The reason for the appearance of lines in the region of large wave numbers in Figure 2 is correct to consider the photoluminescence of intrinsic defects, which are oxygen vacancies, which was already considered earlier for similar materials [6–10].

The ytterbium cation is used in this study, that has its own luminescence [11–15], which allows it to be used as a „probe“ inside the studied oxide. To separate the effects caused by oxygen vacancies, part of the study was performed on oxides doped with yttrium in similar concentrations. Figure 4 shows a comparison of the spectra of cerias doped with one percent of yttrium (top) and ytterbium (bottom). The triplet of the proper lines of the ytterbium cation is clearly visible; however, we note the presence of proper oxide lines in this region of wave numbers (Figure 4, *a*).

As the concentration of ytterbium increases (Figure 5):

- for the spectra obtained in a red laser, the intensity of the ytterbium luminescence lines increases, and their width increases (see Figure 2, *a* and 5, *a*);
- for the spectra obtained in a green laser (cf. Figure 2, *b* and 5, *b*), the reliability of the separation of photoluminescence reflections increases, although their intensity remains low;
- in the region of small wavenumbers, i. e. structural lines, the difference between the structure and pure fluorite, which is characterized by a single band near 460 cm^{-1}, is becoming more pronounced.

As discussed in Ref. [2], the identification of Raman reflections as structural for materials with a high concentration of anionic vacancies is difficult due to the significant photoluminescence caused by these vacancies. The solution is to use radiation sources with different wavelengths: the structural lines do not depend on the wavelength of the radiation used. This approach is used to isolate structural lines, the wave numbers of which, depending on the concentration of ytterbium, are shown in Figure 6. The red diamonds represent a band of the fluorite structure, the wave frequencies of which gradually decrease with the concentration of ytterbium. Even at low concentrations of dopant, weak intensity bands near 600 cm^{-1} are observed (green triangles in Figure 6). Their intensity increases with the concentration of dopant, and after 10 % ytterbium, three lines of the pyrochlore structure can be isolated, as described earlier [2].

Figure 7 shows the concentration dependence of the wavenumbers of the luminescence of the ytterbium cation when the material is irradiated with a laser with a wavelength of 785 nm. In all cases, a triplet is observed, only at low concentrations of the additive, the frequency of the midline is 2375(1) cm^{-1} (Figure 7, *a*) and does not depend on the concentration, and in the area of dopant concentra-

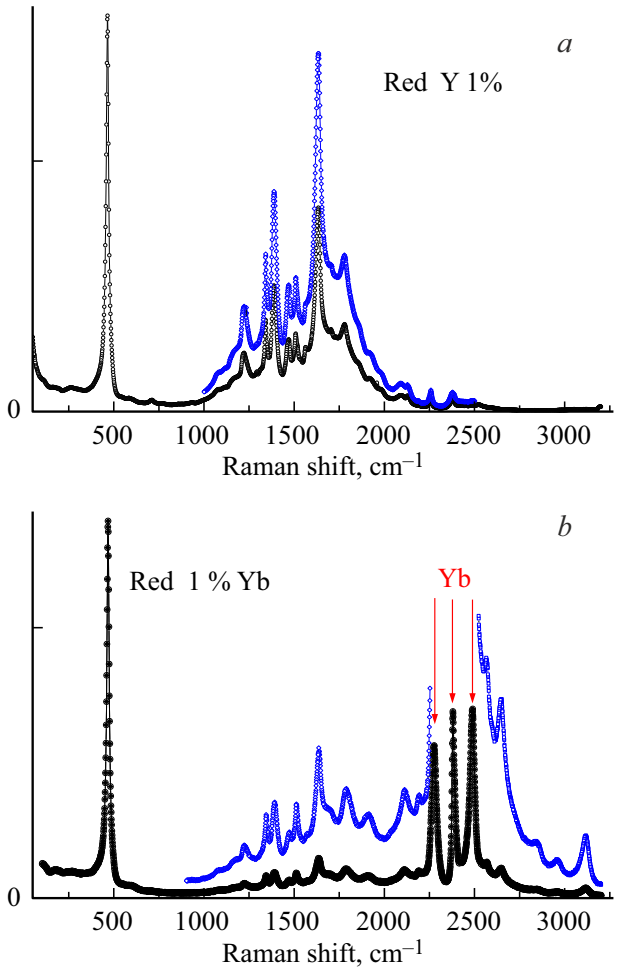

Figure 4. Raman spectra for ceria doped with 1 mol.% *a*) yttrium and *b*) ytterbium obtained using red (785 nm) radiation. The colored lines show the results of shooting with increased exposure.

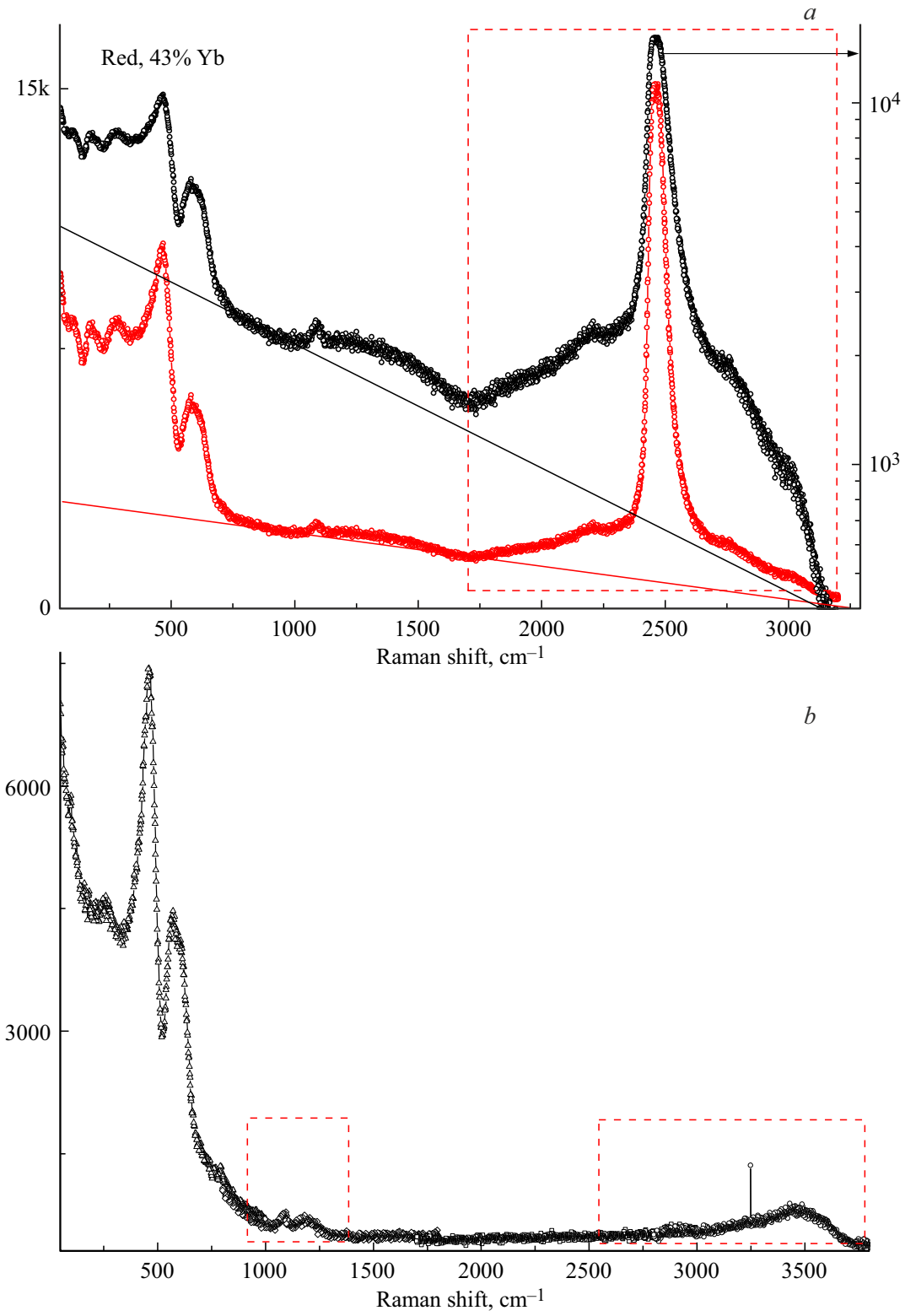

Figure 5. Raman spectra of ceria doped with 43.5 mol.% ytterbium, obtained using *a*) red (785 nm) and *b*) green (532 nm) radiation.

tion is more than 10 % (Figure 7, *b*) is 2440(2) cm^{-1} and also does not depend on the concentration of dopant. The latter value agrees well for derivatives based on zirconium dioxide [9].

The behavior shown in Figure 7 indicates an abrupt change in properties, apparently as a result of a change in the local structure. This correlates well with the results of Figure 6.

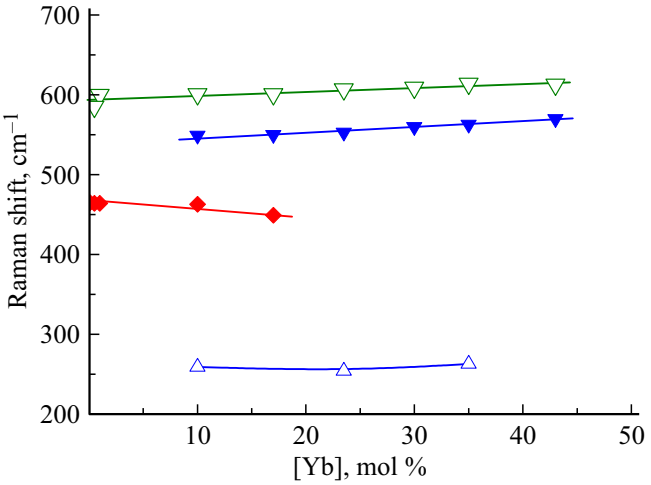

Figure 6. Concentration dependence of the spectral lines of Raman scattering of light, which are reliably structural.

Two types of FCC structures that are not distinguishable by X-ray diffraction methods are structures such as fluorite and pyrochlore, which are implemented for these materials. The transition from the fluorite structure to the pyrochlore structure can be described as the substitution of a trivalent cation for a trivalent one, which leads to the formation of a Yb_{Ce} substitution defect and charge compensation by forming an oxygen vacancy (one vacancy per two substitution acts). As long as the trivalent cations are randomly distributed across the fluorite lattice sites, it is, from the point of view of X-ray diffraction, just a derivatives. And only when a superstructure appears in the position of these defects, it becomes a „ordered derivatives“ with additional diffraction lines. The proportion of dopant in this case should reach 50 % of cations.

Everything is more complicated with the symmetry of the near environment, which is sensitive to the concentration of anionic vacancies. In the fluorite structure itself, the proportion of anionic vacancies is not small, and doping creates more and more vacancies. It is assumed that at high temperatures all oxygen vacancies are delocalized and mobile. On the one hand, the defect interaction energy is estimated at several tenths of eV, which is not small; on the other hand, the room temperature at which Raman spectra are recorded is not high. This means that oxygen vacancies form bound states, leading to a change in local symmetry, which we see. In the pyrochlore structure, where cations of two grades are present, there are 7 allowed Raman structural lines. One of the lines characteristic of the pyrochlore structure is seen in Figure 6, but in the region of very low concentrations of dopant. This suggests that the band near 600 cm^{-1} is due to the bound state of the oxygen vacancy and the cerium cation.

The transition between the structures of fluorite and pyrochlore, even if the local symmetry is considered, turns out to be blurred (Figure 6): the intensity of the line of one structure decreases and the intensity of the lines of the other structure increases. It can be said that at 10 % dopant, the local structure is already predominantly pyrochlore (Figure 6).

The photoluminescence lines of the ytterbium cation turned out to be an unexpectedly bright marker: the frequency of the main line for the fluorite structure at low concentrations of the additive is 2375(1) cm^{-1}, which corresponds to the position of the ytterbium cation in the

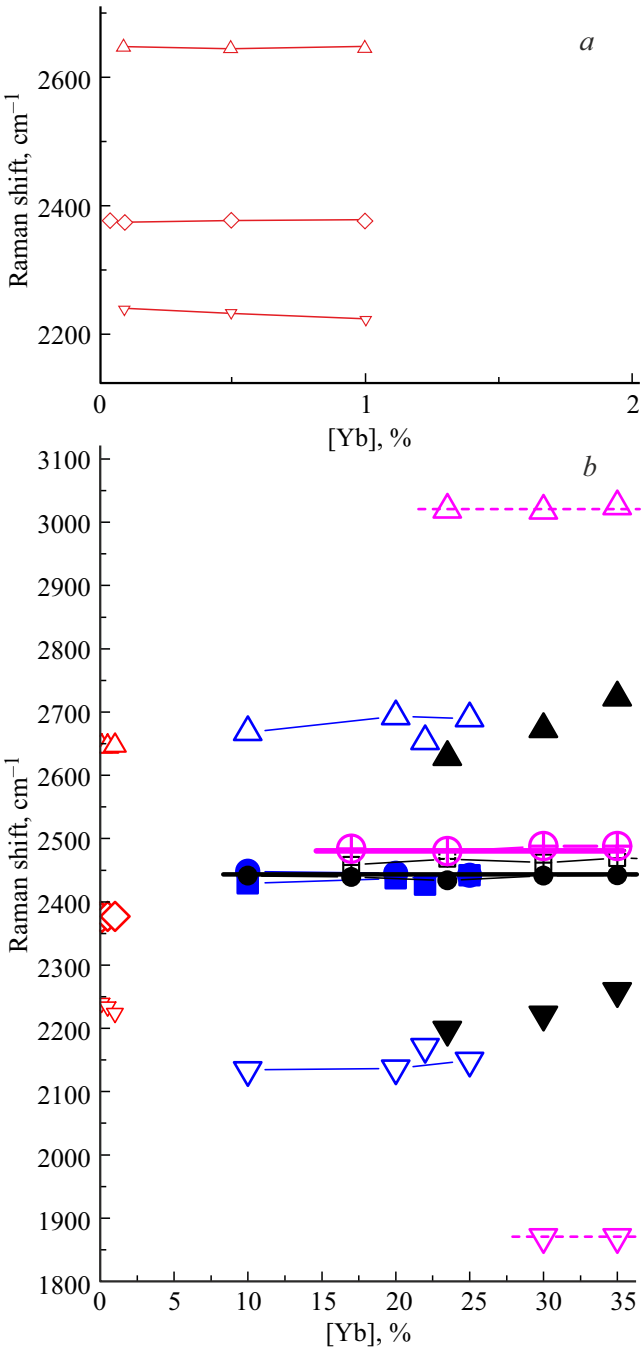

Figure 7. Concentration dependence of the wavenumbers of the luminescence of the ytterbium cation when the material is irradiated with a laser with a wavelength of 785 nm. Black, shaded dots — literature data. Triangular symbols show satellite lines.

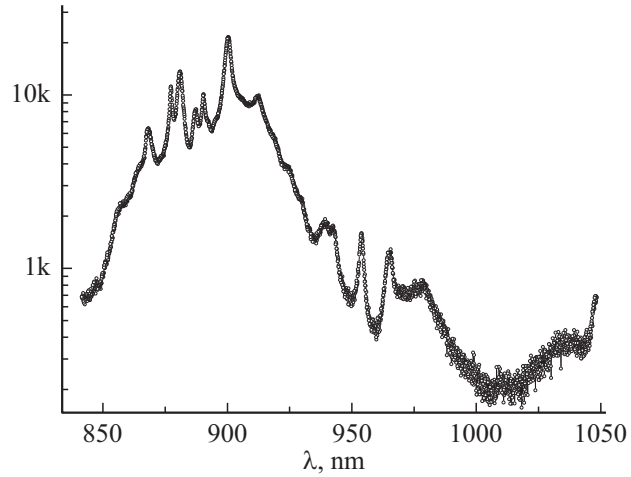

Figure 8. Photoluminescence spectrum of undoped ceria from the region 860−3200 cm^{-1}, rearranged in wavelength coordinates.

ceria matrix without contact with another ytterbium cation. The closest distance between the nodes is half of the diagonal of the face ⟨110⟩. According to Table 1, this value is close to 0.38 nm.

As cerium cations are replaced in one of the 12 positions by ytterbium (8.3 % of the dopant), each ytterbium cation has at least one more ytterbium cation in the neighborhood at a distance of 0.38 nm. The frequency of the main luminescence line of the ytterbium cation is 2440(2) cm^{-1}. The latter value is similar to that for derivatives based on zirconium dioxide (Figure 7, *b*).

The results of Figure 7, *b* allow us to expect that when filling two adjacent positions (about 16 % of the dopant), the central line of the triplet shifts slightly towards high wave numbers, however, the lateral lines of the triplet scatter significantly more (Figure 7, *b*, purple curves); this part of the issue requires a separate detailed study.

Figure 8 shows the photoluminescence spectrum of undoped ceria, rearranged in wavelength coordinates. Obviously, this photoluminescence is caused by oxygen vacancies. A separate report will be devoted to a detailed discussion of the features of this photoluminescence.

4. Conclusion

Thermolysis of formate precursor complexes in air has produced a number of Ce(Yb) derivatives of $Ce(Yb)O_2$, and for selected compositions and $Ce(Y)O_2$. All samples are characterized by a FCC structure (Fm-3m) of the fluorite type.

Raman spectroscopy studies using two different sources (785 and 532 nm) made it possible to identify structural lines and photoluminescence lines, since the structural lines do not depend on the wavelength of the radiation used. Photoluminescence is observed both from the ytterbium cation and from the intrinsic defects of the oxide lattice — anionic vacancies.

A change in the local structure from fluorite to pyrochlore has been traced, it occurs in the region of 9 % of the doping cation and manifests itself not only in a change in the set of structural lines, but also in a change in the frequency of luminescence of the ytterbium cation: 2375(1) cm^{-1} for the fluorite structure at low concentrations of the additive and 2440(2) cm^{-1} for the pyrochlore structure. The latter value agrees well for derivatives based on zirconium dioxide, which also have a pyrochlore structure.

Acknowledgments

The study was performed using the equipment at the Shared Access Center of the Institute of High Temperature Electrochemistry of the Ural Branch of RAS. M.A. Shikhaleeva participated in this study, who at the time of the work was an employee of the IHTE Ural Branch of the Russian Academy of Sciences. The authors are grateful to T.V. Yaroslavtseva, PhD in Chemistry, who was an employee of the Institute of Solid State Chemistry of the Ural Branch of the Russian Academy of Sciences at the time of the study.

Conflict of interest

The authors declare that they have no conflict of interest.

References

[1] V.G. Keramidas, W.B. White. J. Chem. Phys. **59**, *3*, 1561 (1973).
[2] S.N. Shkerin, E.S. Ul'yanova, E.G. Vovkotrub. Inorg. Mater. **57**, *11*, 1145 (2021).
[3] S.N. Shkerin, A.N. Meshcherskikh, T.V. Yaroslavtseva, R.K. Abdurakhimova. Phys. Solid State **64**, *12*, 1951 (2022).
[4] A.C. Cabral, L.S. Cavalcante, R.C. Deus, E. Longo, A.Z. Simões, F. Moura. Ceram. Int. **40**, *3*, 4445 (2014). https://doi.org/10.1016/j.ceramint.2013.08.117
[5] S.N. Shkerin, R.K. Abdurakhimova, P.N. Mushnikov. Neorgan. materialy **61**, *9–10*, 582 (2025) (in Russian). DOI: 10.7868/S3034558825050063
[6] N.G. Petrik, D.P. Taylor, T.M. Orlando. J. Appl. Phys. **85**, *9*, 6770 (1999). https://doi.org/10.1063/1.370192
[7] W.S.C. de Sousa, D.M.A. Melo, J.E.C. da Silva, R.S. Nasar, M.C. Nasar, J.A. Varela. Cerâmica **53**, 99 (2007). https://doi.org/10.1590/S0366-69132007000100015
[8] K. Smits, L. Grigorjeva, D. Millers, A. Sarakovskis, J. Grabis, W. Lojkowski. J. Luminescence **131**, *10*, 2058 (2011). https://doi.org/10.1016/j.jlumin.2011.05.018
[9] S.N. Shkerin, E.S. Ulyanova, E.G. Vovkotrub. Phys. Solid State **64**, *4*, 463 (2022).
[10] S.N. Shkerin, A.V. Pavlovich, R.K. Abdurakhimova, T.V. Yaroslavtseva, E.S. Ulyanova. FTT **66**, *3*, 413 (2024) (in Russian).

[11] Yu.K. Voron'ko, B.I. Denker, V.V. Osiko. FTT **13**, *8*, 2193 (1971) (in Russian).
[12] T. Kallel, M.A. Hassairi, M. Dammak, A. Lyberis, P. Gredin, M. Mortier. J. Alloys Compd. **584**, 261 (2014).
[13] W. Tang, Y. Wang, C.-L. Jia. PhSS **63**, *1*, 110 (2021).
[14] Z. Li, S. Zhang, Q. Xu, D. He, Y. Lv, X. Lin, C. Wang, Y. Jin, Y. Hu. J. Alloys Compd. **766**, 663 (2018).
[15] R. Khabibrakhmanov, A. Shurukhina, A.V. Rudakova, D. Barinov, V. Ryabchuk, A.V. Emeline, G.V. Kataeva, N. Serpone. Chem. Phys. Lett. **742**, *1*, 137136 (2020).

Translated by A.Akhtyamov